Live Cell Plasma Membranes Do Not Exhibit a Miscibility Phase Transition over a Wide Range of Temperatures

Il-Hyung Lee[†], Suvrajit Saha[§], Anirban Polley[#], Hector Huang[†], Satyajit Mayor[§] Madan Rao[§,#] and Jay T. Groves[†,‡*]

[†]*Department of Chemistry, California Institute for Quantitative Biosciences (QB3), Howard Hughes Medical Institute, University of California Berkeley, CA 94720, USA*

[‡]*Materials Sciences Division, Physical Biosciences Division, Lawrence Berkeley National Laboratory, Berkeley, CA 94720, USA*

[§]*National Centre for Biological Sciences (TIFR), Bellary Road, Bangalore 560065, India,*

[#]*Raman Research Institute, C.V. Raman Avenue, Bangalore 560080, India*

[*]*To whom correspondence should be addressed. E-mail: JTGroves@lbl.gov*

Abstract

Lipid:cholesterol mixtures derived from cell membranes, as well as their synthetic reconstitutions, exhibit well defined miscibility phase transitions and critical phenomena near physiological temperatures. This suggests that lipid:cholesterol-mediated phase separation plays a role in the organization of live cell membranes. However, macroscopic lipid phase separation is not generally observed in cell membranes and the degree to which properties of isolated lipid mixtures are preserved in the cell membrane remain unknown. A fundamental property of phase transitions is that the variation of tagged particle diffusion with temperature exhibits an abrupt change as the system passes through the transition, even when the two phases are distributed in a nanometer-scale emulsion. We support this using a variety of Monte-Carlo and atomistic simulations on model lipid membrane systems. However, temperature dependent fluorescence correlation spectroscopy of labeled lipids and membrane-anchored proteins in live cell membranes show a consistently smooth increase of the diffusion coefficient as a function of temperature. We find no evidence of a discrete miscibility phase transition throughout a wide range of temperatures: 14 – 37 °C. This contrasts the behavior of giant plasma membrane vesicles (GPMVs) blebbed from the same cells, which do exhibit phase transitions and macroscopic phase separation. Fluorescence lifetime analysis of a DiI probe in both cases reveals a significant environmental difference between the live cell and the GPMV. Taken together, these data suggest the live cell membrane may avoid the miscibility phase transition inherent to its lipid constituents by actively regulating physical paramters, such as tension, in the membrane.

Keywords: FCS, Fluorescence correlation spectroscopy, Lipid raft, Lipid phase, Membrane diffusion

Introduction

Binary liquid phase separation and miscibility phase transitions in lipid bilayer membranes have been well characterized in ternary mixtures of lipids and cholesterol.[1-6] These membrane systems are widely considered as model systems that mimic the composition of the general mammalian cell plasma membrane. Observations of the same macroscopic miscibility transitions in cell membrane blebs provide compelling confirmation that this is an inherent property of cell membrane lipids.[7-8] Although inhomogeneous lipid interactions have been detected by various high resolution techniques,[9-11] macroscopic phase separation is not generally observed in native living cell membranes. It is possible that cell membrane lipids do exhibit miscibility phase transitions, even in the living cell, but the phase separated domains remain within a nanometer scale as a result of interactions with other cellular structures, such as the cortical actin cytoskeleton. Alternatively, it is also possible that the cytoskeleton, along with other membrane proteins and active cellular processes dominate or even obliterate lipid miscibility effects. The degree to which lipid miscibility phase behavior contributes to the structure of the complete live cell membrane remains controversial.[12-18]

In this report, we measure the collective mobility of a number of membrane components as a function of temperature in living cell membranes by fluorescence correlation spectroscopy (FCS).[19-20] Since collective mobility exhibits a discontinuity as a system passes through a miscibility phase transition,[21-22] these observations are expected to reveal the phase transition, even in cases where the phase domains are too small to resolve by direct imaging. We support this by a variety of Monte-Carlo and atomistic simulations, which show that FCS measurements of tagged particle diffusion would capture such transitions. Our experimental observations, however, consistently reveal a smooth variation of fluorescence autocorrelation time (a measure of collective mobility) with temperature. We find no evidence of a

miscibility transition over the temperature range of 14 – 37°C in the live cell membrane, even though giant plasma membrane vesicles (GPMVs) derived from these same cells do exhibit such transitions.[7] We further investigated the systematic differences between the GPMV and live cell membrane by fluorescence lifetime measurements of the DiI fluorescent probe. The fluorescence lifetime of this probe is sensitive to mechanical aspects (e.g. tension) of the membrane.[23-24] In time-resolved fluorescence measurements, we observe a clear difference in the fluorescence lifetime of the DiI between the living cell and the GPMV. Suggesting the cell membrane may be maintained in a different region of the phase diagram and may even actively avoid a temperature-driven miscibility phase transition. We point out that the lack of a phase transition does not indicate whether or not the membrane is in a phase separated, only that transitions in the live cell membrane cannot be driven by temperature in the 14 – 37°C range.

Methods

Insertion of fluorescence labeled lipids into the live cell membrane

Fluorescently labeled lipid probes were inserted into the cell membrane by incubating RBL2H3 cells grown on clean cover glasses (12-545-102 25CIR-1, Fisher Scientific) with PBS buffer solution containing lipid probes and BSA, as described in detail in previous literature.[8, 10, 25] All fluorescently labeled lipids used for diffusion measurement were labeled with an identical fluorescent probe, BODIPY-FL. Fluorescent lipid analog DiI was used for fluorescence lifetime measurement. The fluorescent probes used were, BODIPY FL C12-sphingomyelin, BODIPY FL C5-ganglioside GM1, BODIPY FL DHPE, β-BODIPY FL C12-HPC, DiIC12(3) and DiIC18(3), all from Invitrogen. Lipid probe incubation was

performed with cells grown on cover glasses preassembled into metal imaging chambers under sterile condition (Attofluor cell chamber, Life Technologies). Natural adherent property of the cell lines stabilized plasma membranes on the glass surface to perform FCS experiments. Only the Jurkat T cell membranes were stabilized by Poly L-Lysine as described below. RBL cells were cultured in DMEM GlutaMAX medium (Gibco) supplemented with 15% fetal bovine serum (FBS, Atlanta Biologicals). Cells were cultured in a T-25 cell culture flask under 37°C, 5% CO_2 condition.

Cloning and Cell Culture/Transfection of anchored GFP fusion proteins

Lipid anchored fluorescent protein constructs were prepared as previously described.[26] Protein constructs were subcloned into the pN1 vector with a strong CMV_{IE} promoter. Full-length and truncated C-Src-GFP fusions (C-Src_{16}-GFP and C-SrcFL-GFP) were engineered from the mouse C-Src gene from Addgene (Plasmid #13663). CD52-GFP genes were gifts from Dr. Björn Lillemeier and Dr. Mark Davis (Stanford University). All oligonucleotides were synthesized by Elim Bioscience (Fremont, CA) and sequenced by Elim Bioscience. Sequence information is provided in the supplementary information.

Jurkat T cells were cultured in RPMI1640 medium (Gibco) supplemented with 1 mM sodium pyruvate (Cellgro), 100 µg/mL Penicillin/Streptomycin (Cellgro), and 10% fetal bovine serum (FBS, Atlanta Biologicals). Cells were passaged every two to three days by seeding ~10^6 cells in 5 mL media in a T-25 cell culture flask and were disposed of after ~15 passages. Cells were transiently transfected 1 day before the experiment by seeding 10^6 Jurkat cells in 2.5 mL Jurkat media and adding transfection mixture of 2.5 µg plasmid DNA mixed with 250 µl Opti-MEM I and 10 µl Lipofectamine 2000 transfection reagent (Invitrogen) incubated at room temperature for 30 min. Transfected cells were incubated at 37°C, 5% CO_2 for ~10-16

h before the FCS experiment.

To prepare transfected Jurkat cells for data acquisition, cell culture media was exchanged twice with 5 mL PBS, pH 7.4 prewarmed to 37°C, by centrifuge (5 min, 250 rcf) and resuspended in 500 µl HEPES buffered saline (pH 7.2) prewarmed to 37°C and deposited on poly-L-lysine coated coverglass (P-L-L, Sigma) enclosed in a metal imaging chamber. Cells were allowed at least 15 min in the incubator in order to settle and adhere to the P-L-L coated coverslips. Effect of P-L-L on membrane anchored protein diffusion is minimal,[24] but it is worth noting that the cells were stabilized by electrostatic interaction between cell membranes and P-L-L. This is different from the method used for other adherent cell lines in which cells were naturally adhered.

Fluorescence Correlation Spectroscopy

FCS was performed on prepared cells with target fluorescent molecules. Spots for measurements were chosen randomly from the bottom membrane of cells with a healthy morphology (Figure 1a). Fluorescent molecules moving in and out of a focused laser spot generated fluctuations of emission intensity, and time-resolved arrival history data of photons collected by a high sensitivity photon detector were recorded (Figure 1b). We looked at three spots per cell and each data point presented here is the ensemble average from ten different cells (n=10, n=5 for anchored protein data). For each spot, five iterations of 10 sec measurements were recorded. A complete set of temperature scanning measurement was performed for each sample by sequentially changing the temperature on the microscope stage. The system was equilibrated for 10 min at each temperature before performing measurements. Each experiment was finished within 2 h 30 min at most from the initial sample preparation. We calculated the time autocorrelation function (Equation 1) from the intensity trace, and

performed function fitting with an anomalous two dimensional diffusion model (Equation 2) to calculate the average decaying time of the correlation function (Figure 1c).[27] An anomalous exponent was introduced to properly consider the non-Brownian nature of molecular diffusion in living cells.[28]

$$G(\tau) = \frac{\langle \delta I(t) \delta I(t+\tau) \rangle}{\langle I \rangle^2} \qquad \text{(Equation 1)}$$

$$G(\tau) = 1 + \frac{1}{N\left(1 + (\tau/\tau_d)\right)^{\alpha}} \qquad \text{(Equation 2)}$$

Igor Pro (WaveMetrics, Inc.) was used for function fitting. The obtained average decay times of each lipid at different temperatures were used to calculate diffusion coefficients from the equation $\tau_d = w^2/4D$.[27] In the equation, w denotes the excitation laser spot width, and D denotes the diffusion coefficient. FCS for Figure 2c was conducted similarly by an independent research group using a different instrumental setup, methods, and cell line from those described in the main text here. Details are given in Supporting Information.

FCS experiments were performed on our apparatus constructed in the following way: 479 nm excitation beam from a 40 MHz pulsed diode laser (LDH-P-C-485, PicoQuant, Berlin, Germany) underfilled the 100× TIRF oil objective [NA 1.49 (Nikon Corp., Tokyo, Japan)] to generate a small focal spot on the sample. Laser power, measured before the objective, was 5-10 μW for BODIPY-FL. The laser power used was tested for photo bleaching effect on an immobile lipid bilayer (Table S1). Our FCS measurement time is reasonably shorter than measured photo bleaching time of immobile fluorescent molecules. Notch filtered (Semrock, Rochester, NY) emission light passed through a 50 μm confocal pinhole (Thorlabs, Newton, NJ) was collected after an emission filter (Chroma Technology Corp., Rockingham, VT) by avalanche photodiodes (APDs) (SPCM-AQRH-16, Perkin&Elmer, Canada). A time-

correlated single photon-counting (TCSPC) card (PicoQuant, TimeHarp 200, Berlin, Germany) collected signal from the APDs through a universal router (PRT 400, TTL SPAD router, PicoQuant, Berlin, Germany) to record time resolved photon fluctuation data, from which the autocorrelation function was calculated using a software correlator written in Matlab (The MathWorks, Inc.) in our own lab, based on a multiple tau algorithm.[29-33] FCS excitation spot size was measured for each experiment by measuring the diffusion coefficient of Alexa Fluor 488 (Invitrogen) solution of known diffusion coefficient.[34] Temperature was controlled by a Peltier based temperature controlling device (Physitemp Instruments, Inc., Warner Instruments, LLC) that directly regulates the temperature of the sample mounted in the microscope (Nikon Corp., Tokyo, Japan). The device performed heating/cooling by transferring heat from the metal sample chambers. Sample temperature was measured in real time by a thermocouple immersed near cell adhered surface to measure the true temperature of samples. Thermal equilibrium of the sample was assured for each temperature point of measurements.

Supported lipid bilayer (SLB) for control experiment was prepared following the literature.[35] BODIPY-FL C12HPC (0.005 mol%) in DOPC vesicles were prepared by extrusion in pure water as 2 mg/ml. Samples were extruded nine times through 100 nm pore size filters (Whatman, Florham Park, NJ) at 50°C in a high pressure extruder (Northern Lipids, Burnaby, British Columbia, Canada). SLB was formed by directly rupturing prepared vesicles on piranha etched cover glasses. Twenty microliter of vesicle solution mixed with PBS buffer as 1:1 was placed onto a clean plastic petri dish and a cleaned coverslip was dropped over the droplet. After 45 sec incubation, the SLB on the cover glass was assembled into the sample chamber in water preventing exposure to air.

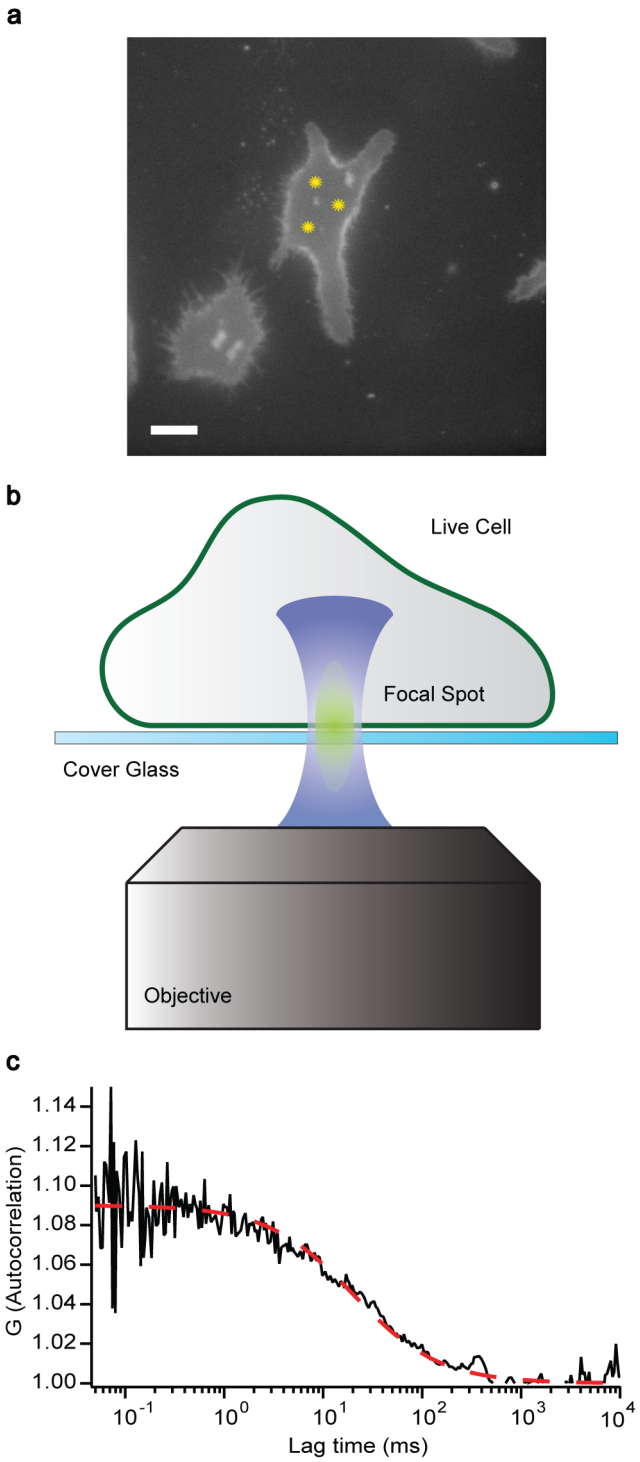

Figure 1: Schematic of the experiment. (a) For each cell, three spots from the bottom plasma membrane were observed. (Marked by yellow spots as an example) Cells with healthy morphology were chosen. (Scale bar 5μm) (b) Cells were grown on the piranha etched cover-glass to fully adhere to the surface. 100x TIRF oil immersion objective focused FCS

excitation spot on the bottom membrane of the live cell. (c) Fitting autocorrelation function of fluorescence fluctuation to two-dimensional anomalous diffusion model enables us to characterize the mobility of the lipid probes.

Fluorescence Lifetime measurement

Fluorescence lifetime measurements were performed with the same setup as FCS measurement but with two photon excitation.[36] Ten seconds of data collection from each spot provided enough signal with a sufficient signal to noise ratio to calculate fluorescence lifetime. A 730 nm, 80 MHz, 100 fs pulsed Titanium:Sapphire laser (Mai Tai HP; Newport Corp, Mountain View, CA) was used as an excitation source. Power before the objective was less than 3mW, which did not cause effective photo bleaching as verified by immobile lipid bilayer measurement (Table S1). Data analysis was done using the SymphoTime software (SymphoTime 5.1.3, PicoQuant, Berlin, Germany). Fitting with the instrument response function (IRF) convoluted lifetime histogram was performed for histograms from each spot. GPMV was prepared following methods from previous literature.[7, 37]

FCS Simulation

Two dimensional Monte-Carlo simulations were performed *in silico* to simulate FCS data with existence of a nano-scale miscibility transition. The data were first collected from simulations, and were then analyzed in the same way as a real experimental case. The only difference was that the samples in this case were virtual fluorescent particles. Matlab (The MathWorks, Inc.) was used for FCS simulations.

First order miscibility transition simulations were performed following the method from the

literature.[11] At each unit time step, virtual fluorescent particles performed random walks with step size determined by a Gaussian random number generator. At higher temperature, mean unit step size was increased as a linear function of temperature. In the phase separated case, particles were given different probabilities for crossing in and out of the domains according to Boltzmann's distribution law. We used exact absolute temperature scaling similar to the actual experimental temperature range to calculate the Boltzmann relation, while temperature used to determine mobility was scaled separately. This is because linear scaling of diffusion in lipid bilayers does not have a zero intercept at absolute zero, as can be seen in our own data, so using the exact absolute scale overestimates the mobility. Properly addressing this issue, we scaled mobility such that it is comparable to the general scaling of two-dimensional lipid diffusion with a negative intercept. Particles were set to move three times slower within the domains.[38] The phase separated terrain was set below the transition temperature of 1.0, while from 1.0 of transition temperature and above, a homogeneous background was assumed. This simulation mimics the immediate formation of domains below the miscibility transition temperature in ternary mixture systems undergoing first order phase transition, but large scale domain coarsening was substituted by nano-scale pattern formation. Domain area was kept constant once formed. What may cause such a result is beyond the scope of our simulation since we are simulating mobility change in a hypothetical case.

Second order miscibility transition simulations were performed on a general two dimensional square lattice Ising model following Kawasaki dynamics similar to previously reported.[39] A small subset of up-spins was assumed to be fluorescent particles. Down-spin particles were chosen three times more often than up-spin particles, which effectively slowed down the up-spin particles. Systems were equilibrated by randomly exchanging spins from any region for enough number of steps to equilibrate the system before starting Kawasaki spin exchange of

neighbors, which was considered as time zero. The spatial resolution of the Kawasaki dynamics was not as high as the first order transition simulation due to the heavy calculation load of Kawasaki dynamics, but the mobility could be sampled out reasonably well with correct simulation of binary fluctuation. The case we studied by first order transition simulation could also be reproduced by this method, supporting the validity of using a smaller discrete Ising model system as virtual FCS samples. Temperature scaling for mobility and inter-particle interaction energy was done the same as the first order transition simulation. A background template was introduced to simulate the near critical fluctuation of the Ising model under the influence of small perturbations. Certain regular positions of the system were assumed to have very favorable interactions with up-spin particles, such that up-spin particles effectively occupied those positions, while still being able to exchange particles with neighboring up-spin particles.

Fluorescence intensity fluctuation was collected by assuming a virtual two dimensional Gaussian excitation spot. Fluorescent particles generated intensity based on a Gaussian profile near the excitation spot position, which was randomly determined. The overall summed intensity at a unit time was then collected assuming a Poisson distribution of detection intensity. Details on parameters used and further figures on simulated systems are given in the Supporting Information.

Atomistic MD Simulation

We used atomistic molecular dynamics (MD) simulations to construct an equilibrated symmetric three component bilayer membrane consisting of 170 Palmitoyl-oleoyl-phosphatidyl-choline (POPC), 171 palmitoyl-sphingomyelin (PSM) and 171 cholesterol, in

the ratio 1:x:x in each leaflet (total 1,024 lipids) and 32,768 water molecules, at 296K. The relative concentration x was varied from 1% to 33%. GROMACS software was used to integrate the equations of motion with a time step of 2 fs. MD simulation details and force fields are given in the Supporting Information. We ensured that the prepared bilayer membrane was mechanically stable, with both the net force and torque balanced, and that the membrane is tensionless.[40-41] In addition, by monitoring the time series of the mean energy and area per lipid (Supporting Information), we ensured that the bilayer was at thermodynamic equilibrium. Equilibrium lateral pressure profiles, for different values of x, are displayed in the Supporting Information. Judicious choice of initial conditions ensured that membrane equilibration occurred quickly. The phase diagram as a function of x was determined and the phase boundary accurately located at x_c = 10%, where a first-order transition occurs between a mixed liquid disordered (ld) phase to a liquid ordered (lo)-ld two-phase coexistence. A variety of physical properties, including the mean square displacement (MSD) of tagged molecules, was studied as a function of x, as one traverses across the phase boundary.

Results

Temperature dependent FCS

Figure 2a shows the diffusion coefficients of four representative lipids as functions of

temperature. Error bars represent the variance originating from both experimental error and inherent heterogeneity of the living cell membrane. The complex nature of live cell membranes resulted in a relatively wider distribution of correlation decay times compared to *in vitro* lipid membrane measurements. Cold shock response of mammalian cells has been studied by many researchers and some suggest change of lipid membrane property.[42-44] If fast lipid trafficking processes[45-46] changing lipid membrane composition in comparable time scale of our measurements were involved in the cold shock response, it would have potentially contributed to the variance too, but intense study on the topic is currently lacking. Inherent variance was the largest in the case of phosphatidylcholine (PC). Nonetheless, the ensemble average value in live cell measurements was reproducible and exhibited a smooth, monotonic increase with temperature for all four different lipids studied. This behavior follows expectation for general particle systems following Einstein behavior: $D=\mu k_B T$, where D is the diffusion coefficient, μ is the molecular mobility, k_B is the Boltzmann constant, and T is the temperature.[47] The relatively slower mobility of sphingomyelin (SM) and GM1 compared to PC and phosphoethanolamine (PE), that we could see in our temperature dependent measurement, has been reported previously and was considered as a signature of nano-scale heterogeneity in the membrane.[10-11, 48] The linear fits of the separate data sets do not differ significantly in slope (Table S2) and, systematic offsets between different lipid species stay constant at different temperatures. It is worth noting that our live cell D(T) data does not conclusively rule out potential Arrhenius dependence from activated hop diffusion,[49-50] and we will keep referring our observed D(T) trend as 'monotonic' without losing general validity of our discussion on discrete phase transition. The Supplementary Information also contains an independent D(T) measurement performed on a different cell line with a different fluorescent analogue measured by two photon FCS (Figure S1). This result adds another example of monotonic D(T) trend.

Control measurements of fluorescent lipids in supported lipid bilayers (SLB) formed on clean glass substrates follow the expected monotonic trend, albeit with a much larger diffusion coefficient than in live cells.[51] This is consistent with free two dimensional Brownian motion driven by thermal fluctuation without the presence of diffusion barriers in the homogeneous supported membrane, and demonstrates the validity of the temperature dependent mobility measurements from our instrumental setup.

Figure 2c shows similar D(T) measurements conducted independently and in parallel with those from Figure 1a and 1b on an entirely different optical setup from a different research group. The same monotonic trend of diffusion coefficients as a function of temperature is conserved with only small differences in absolute values. Seeing the same monotonic increase from two totally independent experiments strongly validates the monotonic behavior of lipid diffusion with respect to temperature as a general lipid behavior in the mammalian cell membrane.

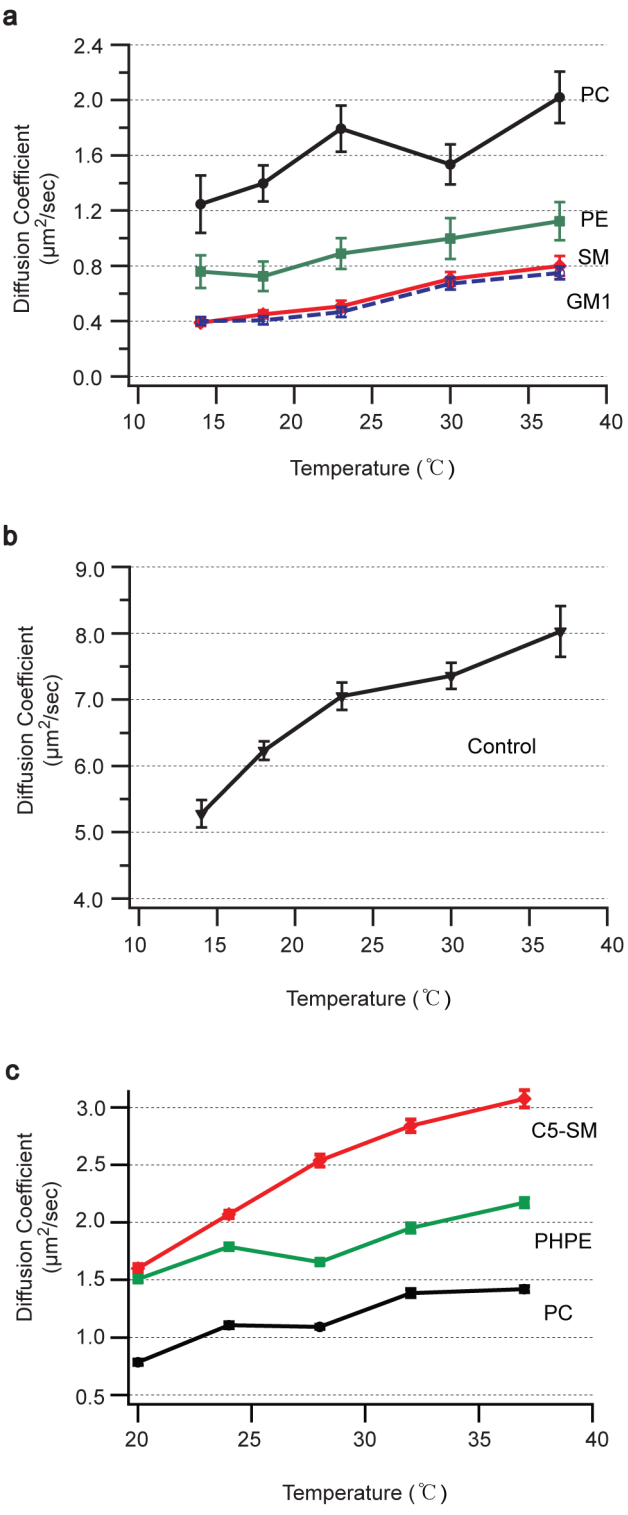

Figure 2: Lipid mobility as a function of temperature. (a) Temperature dependent mobility of four representative lipid probes in the live cell plasma membrane. (RBL2H3 cells) All lipids universally show smooth increase in mobility as functions of temperature with no apparent discontinuity in dD(T)/dT, which is expected in case the system undergoes miscibility

transition. (b) Temperature dependent mobility of the PC probe in DOPC supported lipid bilayer. Monotonic increase of mobility can be seen with much larger absolute value and slope. (c) Similar temperature dependent mobility measurement conducted independently on a different cell line. (CHO cells) Please refer to the supporting information regarding absolute D values of our measurements.

D(T) of membrane anchored proteins

Similar temperature dependent FCS experiments were performed on full-length and truncated forms of membrane anchored protein (i.e., cSrc fused to GFP) in Jurkat T cells (Figure 3). Membrane anchored proteins also exhibited a monotonic increase of diffusion as a function of temperature, showing that the membrane anchored cSrc-GFP proteins in our experiments, also do not undergo any sharp phase transition in this temperature range. Compared to the truncated cSrc anchored GFP (C-Src_{16}-GFP), full length cSrc-GFP (C-SrcFL-GFP) showed systematically slower diffusion at all temperatures, which we propose is because full length proteins are under the influence of more inter-particle interactions on the membrane. Diffusion coefficients of membrane tethered objects are known to mainly depend on viscosity or friction of the lipid membrane.[47, 52-53] This is an example that protein diffusion coefficient as a function of temperature passively follows the behavior of the lipid membrane in live cells. Live cells are expected to impose well controlled perturbation on the membrane to modulate protein diffusion in order to achieve fine control over chemical reactions. An example of such a control is active remodeling of the actin cytoskeleton[54-55] and proteins under the control of such an active process may not follow the similar diffusion coefficient trend as a function of temperature, as the active process may be the dominating factor. Raw autocorrelation decay time data, before calibration with the two-dimensional diffusion model,

are given in Table S3.

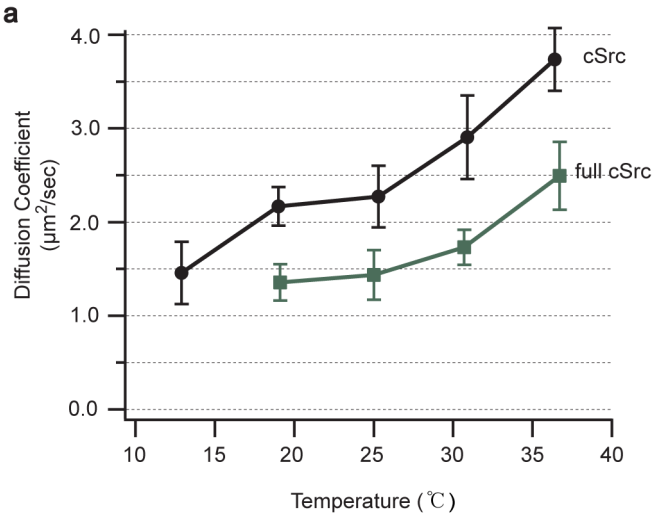

Figure 3: Membrane anchored protein mobility as a function of temperature. Temperature dependent mobility of membrane anchored proteins cSrc-GFP (C-Src_{16}-GFP), full length cSrc-GFP (C-SrcFL-GFP) in the Jurkat T Cell plasma membrane. Diffusion coefficients of both proteins increase smoothly. Full length cSrc proteins show systematically slower mobility compared to cSrc anchor-GFP.

DiI Lifetime measurement

We measured the fluorescence lifetime of DiI, a fluorescent lipid analog, in both living cell membranes and GPMVs derived from it. GPMV was induced following the previously reported method,[8] and we could observe the same miscibility transition as reported. GPMV miscibility transition temperature is known to be dependent on the inducing condition,[56] so it is worth noting that the transition temperature of our GPMV system, induced by

formaldehyde and 2mM dithiothreitol, is around 20°C.[8] The fluorescence lifetime of DiI is linearly correlated with the local viscosity of the dye's surrounding environment, so DiI fluorescence lifetime can be used as membrane tension reporter.[23] We collected data without distinguishing the different phases of phase separated GPMV to correctly mimic the data collection from the cell membrane with hypothetical nano-scale phase separation. Fluorescence lifetime from each TCSPC measurement was calculated by fitting the raw photon arrival histogram to an exponential decaying function convoluted with the measured IRF (Figure 4a). Separate lifetime measurements in live cells with DiIs of different carbon chain lengths, C18 and C12, consistently show an inverse linear response in lifetime as a function of temperature, both in living cell membranes and GPMVs (Figure 4b). DiIC18 and DiIC12 do not differ significantly from each other in lifetime values. The difference in lifetime distribution was not pronounced enough to be considered as a signature of phase transition. DiI lifetimes measured in the two different membrane systems, live cell membranes and GPMVs, show a systematic offset in lifetime, even when GPMVs were originated from the same native plasma membranes. This systematic difference in DiI fluorescence lifetime between two systems suggests clear environmental differences between the two membrane systems. The systematic difference in membrane viscosity between the two systems suggest that the two lipid bilayers are under different membrane tensions, but potential contribution from other factors on fluorescence lifetime difference should be also considered.

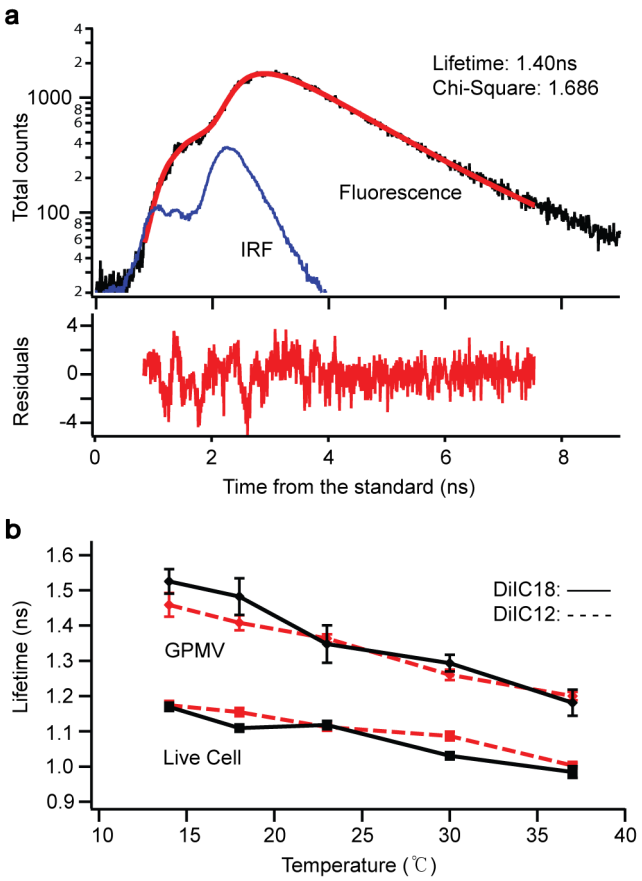

Figure 4: DiI Lifetime increases linearly as temperature is lowered with systematic difference between live cell and GPMV membranes. (a) Fitting schematic of the lifetime data. An exponential decay function convoluted with measured Impulse Response Function (IRF) of the detector was used to fit lifetime histograms obtained by TCSPC. (b) Temperature dependent lifetime of the fluorescent lipid analogue DiIs with different saturated carbon tail length. Lifetime increases as temperature is lowered due to sensitive nature of DiI probe to the membrane viscosity. DiI lifetime shows same inverse linear trend both in live cell and GPMV membranes, but the absolute values are clearly different between two systems. This indicates that GPMVs and live cell membranes are at different physical states.

FCS simulation

We performed Monte Carlo simulations to simulate virtual nanometer-scale phase transition observed by temperature dependent FCS. To serve as a positive control of our temperature dependent FCS experiment, the membrane system should undergo clear reversible miscibility transition at a transition temperature, and phase separation should occur over a very small scale, such that it is invisible to conventional light microscopy. Availability of such an *in vitro* membrane system for FCS is still ambiguous, despite ongoing effort to study small scale heterogeneity in some membrane systems,[3, 57-58] so we decided to study an *in silico* counterpart of our live cell experiment.

First order transition simulations clearly show a discontinuity of mobility as a function of temperature, as generally expected (Figure 5a). A passive diffusion barrier, mimicking static cytoskeletal structure,[11, 59] imposed on the system does not suppress the existence of this discontinuity. Variations in physical parameters do not eliminate this discontinuity, thus demonstrating the robustness of this discontinuity. The second order transition case was studied using an Ising model. Near critical fluctuation can cause characteristically different behavior of a system near the transition temperature from that of the first order transition case.[17, 39] In second order transition simulations, introducing a small template to perturb the system, which is similar to the simulation performed in previous literature,[39] was enough to suppress the large scale phase separation below the original critical temperature (Figure S3). In this case, the mobility of virtual up-spin particles shows a linear response as a function of temperature, with no clear discontinuity or change in slope (Figure 5b). This means that, with a small perturbation, a second order miscibility transition can be quenched,[60] effectively making the mobility response appear linear, as if following the Einstein relation. Actin cytoskeletal structure is currently considered as a major source of such a template

interaction,[39, 60] and the glycan network is another template example.[61-62] An experimental case of static actin quenched miscibility transition studied by super resolution FCS was reported recently,[63] although domain fluctuation of the system was still not under the resolution of light microscopy.

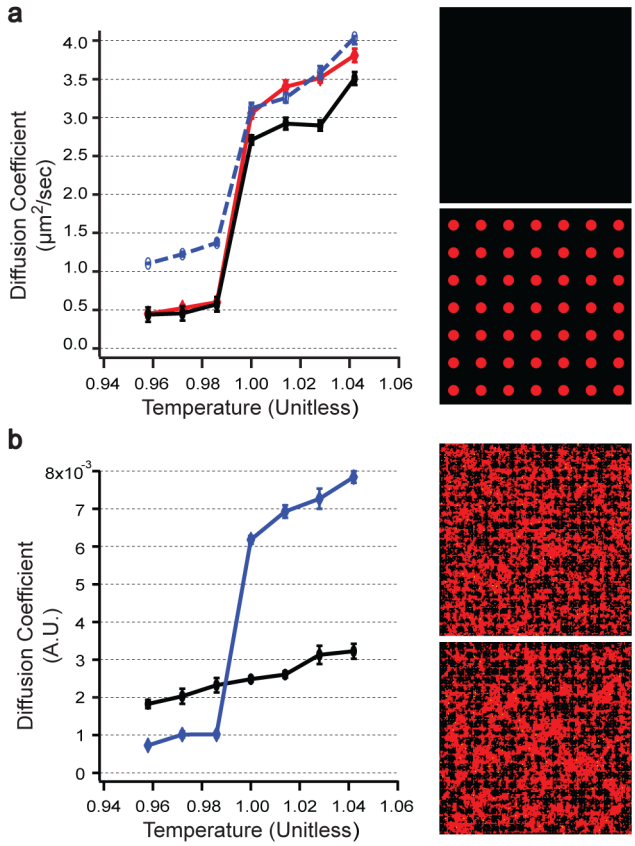

Figure 5: FCS simulation results for first and second order miscibility transition. (a) First order miscibility transition shows clear discontinuity in mobility as a function of temperature. Phase separated state was assumed under T=1.0 (low right) and homogeneous state was assumed from and above it (upper right). Data for 40nm diameter domains with distance of 50nm (red line), 100nm (blue dashed line), and complex terrain with diffusion barriers (black line) are shown. More figures for each system are given in (Fig. S2). (b) Second order miscibility transition under small perturbation shows linear mobility response as a function of temperature (black line). First order transition case could be reproduced using the same

Kawasaki dynamics simulation (blue line). More figures for each system are given in (Fig. S3).

Atomistic MD simulation

In addition, we carried out atomistic molecular dynamics simulations to study how tagged particle diffusion changes across a miscibility transition point. MD simulations were performed on the ternary component, symmetric bilayer membrane containing POPC, PSM and Cholesterol, in both the leaflets (Figure 6a) with varying levels of x, the concentration of PSM (Chol) (Figure 6b). Although this simulation is composition dependent, not temperature dependent scaling, it provides us with an important clue as to how crossing the miscibility transition point affects diffusion of lipids at the atomistic level. Experimental ternary lipid systems undergo miscibility transition both in composition and temperature spaces (Figure 7a, reproduced from the literature[64]). After ensuring thermodynamic equilibrium at late times, we computed the mean square displacement (MSD) of tagged PSM and POPC over a time scale of 100 ns. We averaged over all molecules of the same species. To allow for the possibility of anomalous diffusion, we did a best-fit of MSD data to $\langle \delta r^2 \rangle \propto t^{\alpha}$ (Supplementary Figure S5). We then computed the diffusion coefficient as a function of x. We found that for POPC, a lipid that segregates into ld domains at $x > 10\%$, the diffusion coefficient is a smoothly decreasing function of x with no sharp changes. Whereas for PSM, a lipid that segregates into lo domains at $x > 10\%$, the diffusion coefficient shows a sharp fall across the phase boundary x_c=10% (Figure 6c). The discontinuity observed is similar to that of the first order transition Monte-Carlo simulation (Figure 5), and it supports the expectation of observing a discontinuity in the diffusion coefficient near a miscibility transition point.

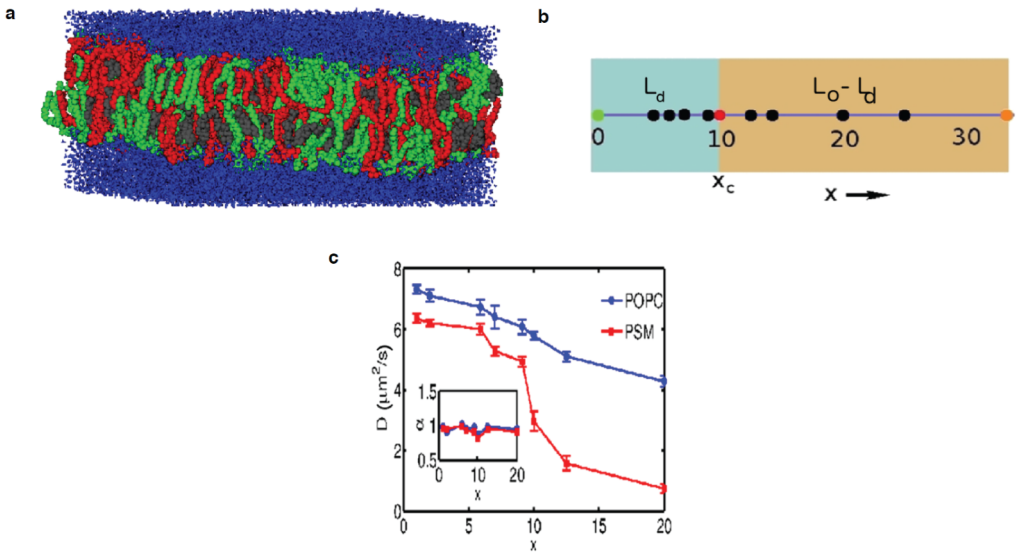

Figure 6: Atomistic MD simulations of ternary component membrane bilayer. (a) Snapshot of MD simulation showing equilibrium configuration of the ternary component symmetric bilayer membrane with POPC (green), PSM (red), Chol (black) in water (blue). 1:x:x in each leaflet (total 1,024 lipids) and 32,768 water molecules, at 296K. (b) Phase diagram as a function of x, the relative concentration of PSM (Chol) showing a phase transition between the ld phase at $x < 10\%$ and the lo-ld coexistence region at $x > 10\%$. The dots indicate the compositions where the simulations were performed. (c) Tagged molecular diffusion of POPC and PSM as x varies across x_c. The mean square displacement (MSD) of a tagged molecule is defined as $< \delta r_i(t)^2 >$, where $\delta r_i(t) = r_i(t) - r_i(0)$ is the displacement of the i^{th} lipid of a given species at time t from its position at t = 0. We fit the MSD to $< \delta r_i(t)^2 > \propto t^{\alpha}$, where α = 1 for ideal Brownian diffusive motion. Inset shows that $\alpha \approx 1$ for all x. Plot of the diffusion coefficients D of POPC and PSM shows that while the diffusion of POPC decreases smoothly as a function of x, the diffusion of PSM shows a sharp jump across $x=x_c=10\%$.

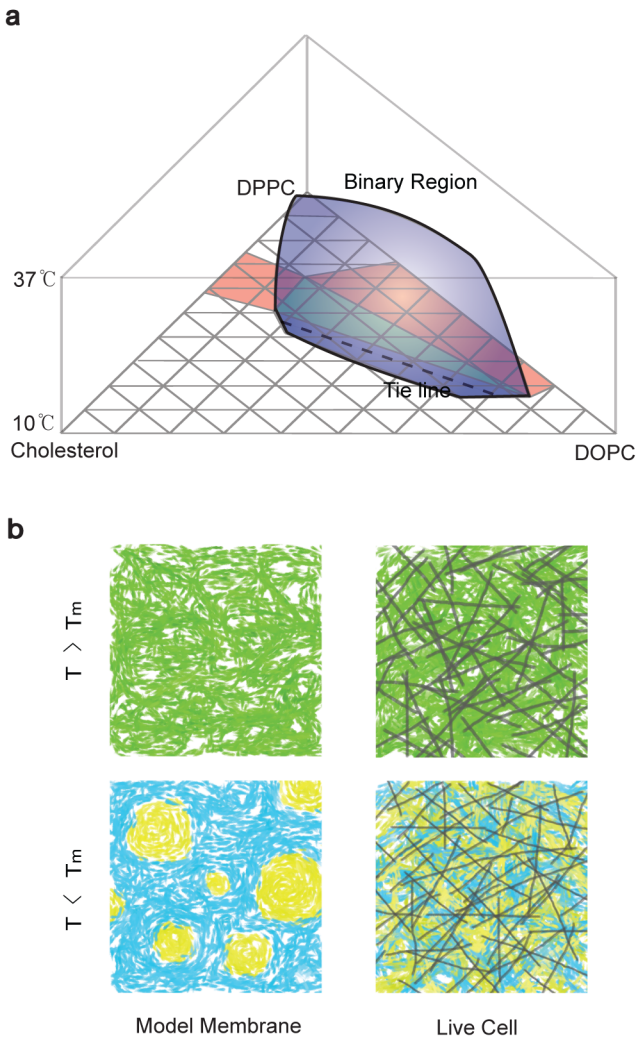

Figure 7: Miscibility transition of the lipid ternary mixture system and hypothetical states of the live cell membrane. (a) Lipid ternary mixture system shows reversible temperature dependent miscibility transition at various compositions (surface of the blue Binary region of the diagram). GPMV also shows similar miscibility transition with critical behavior around 23℃. (b) Comparison of the model membrane and its live cell membrane counterpart at different states. Two hypothetical states can be assumed for the live cell membrane. One case is that it is under the transition temperature. In this case, the spatial scale of the inhomogeneity has to be smaller than optical limit which prevents us from observing it experimentally. (Lower right) This means very finely dispersed two dimensional immersion state of the lipid membrane. Another case is that it is above the transition temperature where

the membrane is in a single homogeneous phase. (Upper right) Actin cytoskeletal structure, the major source of template interaction, is drawn as gray lines. Yellow and blue regions denote two different lipid phases. Green regions denote a single homogeneous lipid phase. White space was introduced only for artistic purposes and do not specify any molecule.

Conclusion

Here we have presented a wide range of measurements on live cell membranes, conducted by independent research teams on opposite sides of the world, that confirm a smooth monotonic scaling of molecular diffusion coefficient with temperature (14-37 °C). Despite the fact that lipid mixtures directly extracted from cells exhibit miscibility phase transitions around room temperature,[7-8] no such transition is observed in the live cell. These results do not indicate whether the membrane is phase separated or homogeneous, only that whichever state it is in appears to be maintained over the entire temperature range studied. A systematic difference in DiI fluorescence lifetime between GPMVs and live cell membranes reveals a difference in the membrane environment of the two systems.[23] The differential physical state, presumably tension, could be caused by the live cell plasma membrane's interaction with cortical actin[55, 65] and may shift the plasma membrane to a point in the phase diagram where the miscibility transition temperature is lower.[66] However, an absolute magnitude of such tension in live cells may be insufficient to consider tension as the sole principle suppressing miscibility phase transition,[67] and template quenched second order miscibility transition,[39, 60, 63] as observed in our simulations, may deserve more attention. Perturbation by active processes,[37, 55, 68-69] for physiological function, will add even more complexity to the membrane

organization. Figure 7b shows hypothetical states of the live cell membrane. Our result suggests the cell membrane maintains either the ($T > T_m$) or ($T < T_m$) case throughout the wide range of temperatures studied. This adds a further example of the robustness of biological systems against environmental change.

Acknowledgement

We acknowledge Prof. Adam Smith for help in experimental design and optical alignment. We also acknowledge Dr. Christopher Rhodes and Dr. Michael Coyle for FCS data analysis and Ann Fischer from UC Berkeley Tissue Culture Facility for mammalian cell cultures. We thank Prof. Sarah Veatch for kindly providing the data we used for Figure 7a ternary mixture phase diagram. This work was supported by the Director, Office of Science, Office of Basic Energy Sciences, of the U.S. Department of Energy under Contract No. DE-AC02-05CH11231.

Supporting Information Available

Extended methods, supporting tables and figures. This information is available free of charge via the Internet at http://pubs.acs.org.

References

(1) Veatch, S. L.; Keller, S. L., Separation of Liquid Phases in Giant Vesicles of Ternary Mixtures of Phospholipids and Cholesterol. *Biophys. J.* **2003**, *85*, 3074-83.
(2) Blosser, Matthew C.; Starr, Jordan B.; Turtle, Cameron W.; Ashcraft, J.; Keller, Sarah L., Minimal Effect of Lipid Charge on Membrane Miscibility Phase Behavior In three Ternary Systems. *Biophys. J.* **2013**, *104*, 2629-2638.
(3) Heberle, F. A.; Wu, J.; Goh, S. L.; Petruzielo, R. S.; Feigenson, G. W., Comparison of Three Ternary Lipid Bilayer Mixtures: Fret and Esr Reveal Nanodomains. *Biophys. J.* **2010**, *99*, 3309-18.
(4) Heinrich, M.; Tian, A.; Esposito, C.; Baumgart, T., Dynamic Sorting of Lipids and Proteins in Membrane Tubes with a Moving Phase Boundary. *Proc. Natl. Acad. Sci. U.S.A.* **2010**, *107*, 7208-7213.
(5) Ionova, Irina V.; Livshits, Vsevolod A.; Marsh, D., Phase Diagram of Ternary Cholesterol/Palmitoylsphingomyelin/Palmitoyloleoyl-Phosphatidylcholine Mixtures: Spin-Label Epr Study of Lipid-Raft Formation. *Biophys. J.* **2012**, *102*, 1856-1865.
(6) Bezlyepkina, N.; Gracià, R. S.; Shchelokovskyy, P.; Lipowsky, R.; Dimova, R., Phase Diagram and Tie-Line Determination for the Ternary Mixture Dopc/Esm/Cholesterol. *Biophys. J.* **2013**, *104*, 1456-1464.
(7) Baumgart, T.; Hammond, A. T.; Sengupta, P.; Hess, S. T.; Holowka, D. A.; Baird, B. A.; Webb, W. W., Large-Scale Fluid/Fluid Phase Separation of Proteins and Lipids in Giant Plasma Membrane Vesicles. *Proc. Natl. Acad. Sci. U.S.A.* **2007**, *104*, 3165-70.
(8) Veatch, S. L.; Cicuta, P.; Sengupta, P.; Honerkamp-Smith, A.; Holowka, D.; Baird, B., Critical Fluctuations in Plasma Membrane Vesicles. *ACS Chem. Biol.* **2008**, *3*, 287-93.
(9) Sahl, S. J.; Leutenegger, M.; Hilbert, M.; Hell, S. W.; Eggeling, C., Fast Molecular Tracking Maps Nanoscale Dynamics of Plasma Membrane Lipids. *Proc. Natl. Acad. Sci. U.S.A.* **2010**, *107*, 6829-34.
(10) Eggeling, C., et al., Direct Observation of the Nanoscale Dynamics of Membrane Lipids in a Living Cell. *Nature* **2009**, *457*, 1159-62.
(11) Wawrezinieck, L.; Rigneault, H.; Marguet, D.; Lenne, P. F., Fluorescence Correlation Spectroscopy Diffusion Laws to Probe the Submicron Cell Membrane Organization. *Biophys. J.* **2005**, *89*, 4029-42.
(12) Fan, J.; Sammalkorpi, M.; Haataja, M., Formation and Regulation of Lipid Microdomains in Cell Membranes: Theory, Modeling, and Speculation. *FEBS Lett.* **2010**, *584*, 1678-1684.
(13) Lingwood, D.; Simons, K., Lipid Rafts as a Membrane-Organizing Principle. *Science* **2010**, *327*, 46-50.
(14) Sengupta, P.; Baird, B.; Holowka, D., Lipid Rafts, Fluid/Fluid Phase Separation, and Their Relevance to Plasma Membrane Structure and Function. *Semin. Cell. Dev. Biol.* **2007**, *18*, 583-590.
(15) Pike, L. J., The Challenge of Lipid Rafts. *J. Lipid. Res.* **2009**, *50*, S323-S328.
(16) Heberle, F. A.; Feigenson, G. W., Phase Separation in Lipid Membranes. *Cold. Spring. Harb. Perspect. Biol.* **2011**, 3, a004630.
(17) Honerkamp-Smith, A. R.; Veatch, S. L.; Keller, S. L., An Introduction to Critical Points for Biophysicists; Observations of Compositional Heterogeneity in Lipid Membranes. *Biochim. Biophys. Acta* **2009**, *1788*, 53-63.
(18) Mayor, S.; Rao, M., Rafts: Scale-Dependent, Active Lipid Organization at the Cell Surface. *Traffic* **2004**, *5*, 231-240.
(19) Magde, D.; Elson, E.; Webb, W. W., Thermodynamic Fluctuations in a Reacting System—Measurement by Fluorescence Correlation Spectroscopy. *Phys. Rev. Lett.* **1972**, *29*, 705-708.
(20) Groves, J. T.; Parthasarathy, R.; Forstner, M. B., Fluorescence Imaging of Membrane Dynamics. *Annu. Rev. Biomed. Eng.* **2008**, *10*, 311-338.
(21) Kahya, N.; Scherfeld, D.; Bacia, K.; Schwille, P., Lipid Domain Formation and Dynamics in Giant Unilamellar Vesicles Explored by Fluorescence Correlation Spectroscopy. *J. Struct. Biol.* **2004**, *147*, 77-89.
(22) Levental, I.; Byfield, F. J.; Chowdhury, P.; Gai, F.; Baumgart, T.; Janmey, P. A., Cholesterol-Dependent Phase Separation in Cell-Derived Giant Plasma-Membrane Vesicles. *Biochem. J.* **2009**, *424*, 163-7.
(23) Tabouillot, T.; Muddana, H. S.; Butler, P. J., Endothelial Cell Membrane Sensitivity to Shear Stress Is Lipid Domain Dependent. *Cell. Mol. Bioeng.* **2011**, *4*, 169-181.
(24) Muddana, H. S.; Gullapalli, R. R.; Manias, E.; Butler, P. J., Atomistic Simulation of Lipid and Dii Dynamics in Membrane Bilayers under Tension. *Phys. Chem. Chem. Phys.* **2011**, *13*, 1368-1378.
(25) Bacia, K.; Scherfeld, D.; Kahya, N.; Schwille, P., Fluorescence Correlation Spectroscopy Relates Rafts in Model and Native Membranes. *Biophys. J.* **2004**, *87*, 1034-43.
(26) Triffo, S. B.; Huang, H. H.; Smith, A. W.; Chou, E. T.; Groves, J. T., Monitoring Lipid Anchor Organization in Cell Membranes by Pie-Fccs. *J. Am. Chem. Soc.* **2012**, *134*, 10833-10842.
(27) Schwille, P.; Korlach, J.; Webb, W. W., Fluorescence Correlation Spectroscopy with Single-Molecule

Sensitivity on Cell and Model Membranes. *Cytometry* **1999**, *36*, 176-82.
(28) Saxton, M. J., A Biological Interpretation of Transient Anomalous Subdiffusion. I. Qualitative Model. *Biophys. J.* **2007**, *92*, 1178-91.
(29) Schätzel, K., Single-Photon Correlation Techniques. *Dynamic Light Scattering,* W. Brown ed; Oxford University: Oxford, U.K., 1993, pp 76-148.
(30) Schätzel, K.; Drewel, M.; Stimac, S., Photon Correlation Measurements at Large Lag Times: Improving Statistical Accuracy. *J. Mod. Opt.* **1988**, *35*, 711-718.
(31) Magatti, D.; Ferri, F., Fast Multi-Tau Real-Time Software Correlator for Dynamic Light Scattering. *Appl. Opt.* **2001**, *40*, 4011-4021.
(32) Schätzel, K., New Concepts in Correlator Design, *Inst. Phys. Conf. Ser*. **1985**, 77, 175-184.
(33) Schätzel, K., Correlation Techniques in Dynamic Light Scattering. *Appl. Phys. B* **1987**, *42*, 193-213.
(34) Nitsche, J. M.; Chang, H.-C.; Weber, P. A.; Nicholson, B. J., A Transient Diffusion Model Yields Unitary Gap Junctional Permeabilities from Images of Cell-to-Cell Fluorescent Dye Transfer between Xenopus Oocytes. *Biophys. J.* **2004**, *86*, 2058-2077.
(35) Lin, W.-C.; Yu, C.-H.; Triffo, S.; Groves, J. T., Supported Membrane Formation, Characterization, Functionalization, and Patterning for Application in Biological Science and Technology. *Curr. Protoc. Chem. Biol.* **2010**, *2*, 235-269.
(36) Berland, K. M.; So, P. T.; Gratton, E., Two-Photon Fluorescence Correlation Spectroscopy: Method and Application to the Intracellular Environment. *Biophys. J.* **1995**, *68*, 694-701.
(37) Fan, J.; Sammalkorpi, M.; Haataja, M., Lipid Microdomains: Structural Correlations, Fluctuations, and Formation Mechanisms. *Phys. Rev. Lett.* **2010**, *104*, 118101.
(38) Dietrich, C.; Bagatolli, L. A.; Volovyk, Z. N.; Thompson, N. L.; Levi, M.; Jacobson, K.; Gratton, E., Lipid Rafts Reconstituted in Model Membranes. *Biophys. J.* **2001**, *80*, 1417-28.
(39) Machta, B. B.; Papanikolaou, S.; Sethna, J. P.; Veatch, S. L., Minimal Model of Plasma Membrane Heterogeneity Requires Coupling Cortical Actin to Criticality. *Biophys. J.* **2011**, *100*, 1668-77.
(40) Polley, A.; Vemparala, S.; Rao, M., Atomistic Simulations of a Multicomponent Asymmetric Lipid Bilayer. *J. Phys. Chem. B* **2012**, *116*, 13403-13410.
(41) Polley, A.; Mayor, S.; Rao, M., Bilayer Registry in a Multicomponent Asymmetric Membrane: Dependence on Lipid Composition and Chain Length. *J. Chem. Phys.* **2014***,* 141, 064903.
(42) Fujita, J., Cold Shock Response in Mammalian Cells. *J. Mol. Microbiol. Biotechnol.* **1999**, *1*, 243-255.
(43) Sonna, L. A.; Fujita, J.; Gaffin, S. L.; Lilly, C. M., Invited Review: Effects of Heat and Cold Stress on Mammalian Gene Expression. *J. Appl. Physiol.* **2002**, *92*, 1725-1742.
(44) Al-Fageeh, M.; Smales, C., Control and Regulation of the Cellular Responses to Cold Shock: The Responses in Yeast and Mammalian Systems. *Biochem. J.* **2006**, *397*, 247-259.
(45) Meer, G., Lipid Traffic in Animal Cells. *Annu. Rev. Cell. Biol.* **1989**, *5*, 247-275.
(46) Hanada, K.; Kumagai, K.; Yasuda, S.; Miura, Y.; Kawano, M.; Fukasawa, M.; Nishijima, M., Molecular Machinery for Non-Vesicular Trafficking of Ceramide. *Nature* **2003**, *426*, 803-809.
(47) Saffman, P. G.; Delbruck, M., Brownian Motion in Biological Membranes. *Proc. Natl. Acad. Sci. U.S.A.* **1975**, *72*, 3111-3113.
(48) Lenne, P.-F.; Wawrezinieck, L.; Conchonaud, F.; Wurtz, O.; Boned, A.; Guo, X.-J.; Rigneault, H.; He, H.-T.; Marguet, D., Dynamic Molecular Confinement in the Plasma Membrane by Microdomains and the Cytoskeleton Meshwork. *EMBO J.* **2006**, *25*, 3245-3256.
(49) Bag, N.; Yap, D. H. X.; Wohland, T., Temperature Dependence of Diffusion in Model and Live Cell Membranes Characterized by Imaging Fluorescence Correlation Spectroscopy. *Biochim. Biophys. Acta, Biomembr.* **2014**, *1838*, 802-813.
(50) Di Rienzo, C.; Gratton, E.; Beltram, F.; Cardarelli, F., Fast Spatiotemporal Correlation Spectroscopy to Determine Protein Lateral Diffusion Laws in Live Cell Membranes. *Proc. Natl. Acad. Sci. U.S.A.* **2013**, *110*, 12307-12312.
(51) Forstner, M. B.; Yee, C. K.; Parikh, A. N.; Groves, J. T., Lipid Lateral Mobility and Membrane Phase Structure Modulation by Protein Binding. *J. Am. Chem. Soc.* **2006**, *128*, 15221-7.
(52) Peters, R.; Cherry, R. J., Lateral and Rotational Diffusion of Bacteriorhodopsin in Lipid Bilayers: Experimental Test of the Saffman-Delbrück Equations. *Proc. Natl. Acad. Sci. U.S.A.* **1982**, *79*, 4317-4321.
(53) Ziemba, B. P.; Li, J.; Landgraf, K. E.; Knight, J. D.; Voth, G. A.; Falke, J. J., Single-Molecule Studies Reveal a Hidden Key Step in the Activation Mechanism of Membrane-Bound Protein Kinase C-A. *Biochemistry* **2014**, *53*, 1697-1713.
(54) Chaudhuri, A.; Bhattacharya, B.; Gowrishankar, K.; Mayor, S.; Rao, M., Spatiotemporal Regulation of Chemical Reactions by Active Cytoskeletal Remodeling. *Proc. Natl. Acad. Sci. U.S.A.* **2011**, *108*, 14825-14830.
(55) Gowrishankar, K.; Ghosh, S.; Saha, S.; C, R.; Mayor, S.; Rao, M., Active Remodeling of Cortical Actin Regulates Spatiotemporal Organization of Cell Surface Molecules. *Cell* **2012**, *149*, 1353-1367.

(56) Levental, I.; Grzybek, M.; Simons, K., Raft Domains of Variable Properties and Compositions in Plasma Membrane Vesicles. *Proc. Natl. Acad. Sci. U.S.A.* **2011**, *108*, 11411-6.
(57) Brown, A. C.; Wrenn, S. P., Nanoscale Phase Separation in Dspc–Cholesterol Systems. *Langmuir* **2013**, *29*, 9832-9840.
(58) Suga, K.; Umakoshi, H., Detection of Nanosized Ordered Domains in Dopc/Dppc and Dopc/Ch Binary Lipid Mixture Systems of Large Unilamellar Vesicles Using a Tempo Quenching Method. *Langmuir* **2013**, *29*, 4830-4838.
(59) Murase, K.; Fujiwara, T.; Umemura, Y.; Suzuki, K.; Iino, R.; Yamashita, H.; Saito, M.; Murakoshi, H.; Ritchie, K.; Kusumi, A., Ultrafine Membrane Compartments for Molecular Diffusion as Revealed by Single Molecule Techniques. *Biophys. J.* **2004**, *86*, 4075-93.
(60) Fischer, T.; Vink, R. L. C., Domain Formation in Membranes with Quenched Protein Obstacles: Lateral Heterogeneity and the Connection to Universality Classes. *J. Chem. Phys.* **2011**, 055106.
(61) Groves, J. T., Cell Membranes: Glycans' Imprints. *Nat. Mater.* **2013**, *12*, 96-97.
(62) Subramaniam, A. B.; Guidotti, G.; Manoharan, V. N.; Stone, H. A., Glycans Pattern the Phase Behaviour of Lipid Membranes. *Nat. Mater.* **2013**, *12*, 128-133.
(63) Honigmann, A.; Sadeghi, S.; Keller, J.; Hell, S. W.; Eggeling, C.; Vink, R., *A Lipid Bound Actin Meshwork Organizes Liquid Phase Separation in Model Membranes*, **2014**, Elife, 3, e01671.
(64) Veatch, S. L.; Soubias, O.; Keller, S. L.; Gawrisch, K., Critical Fluctuations in Domain-Forming Lipid Mixtures. *Proc. Natl. Acad. Sci. U.S.A.* **2007**, *104*, 17650-5.
(65) Dai, J.; Sheetz, M. P., Membrane Tether Formation from Blebbing Cells. *Biophys. J.* **1999**, *77*, 3363-3370.
(66) Uline, Mark J.; Schick, M.; Szleifer, I., Phase Behavior of Lipid Bilayers under Tension. *Biophys. J.* **2012**, *102*, 517-522.
(67) Portet, T.; Gordon, Sharona E.; Keller, Sarah L., Increasing Membrane Tension Decreases Miscibility Temperatures; an Experimental Demonstration Via Micropipette Aspiration. *Biophys. J.* **2012**, *103*, L35-L37.
(68) Sens, P.; Turner, M. S., Microphase Separation in Nonequilibrium Biomembranes. *Phys. Rev. Lett.* **2011**, *106*, 238101.
(69) Fan, J.; Sammalkorpi, M.; Haataja, M., Domain Formation in the Plasma Membrane: Roles of Nonequilibrium Lipid Transport and Membrane Proteins. *Phys. Rev. Lett.* **2008**, *100*, 178102.

TOC Imag